RSC Advances

Accepted Manuscript

This article can be cited before page numbers have been issued, to do this please use: M. Singh and O. Silakari, *RSC Adv.*, 2016, DOI: 10.1039/C6RA17678J.

ROYAL SOCIETY OF CHEMISTRY

rsc.li/rsc-advances

View Article Online
DOI: 10.1039/C6RA17678J

Design, Synthesis and Biological Evaluation of Novel 2-phenyl-1-benzopyran-4-one Derivatives as Potential Poly-functional Anti-Alzheimer's Agents

Manjinder Singh[a], Om Silakari[a,*]

[a] *Molecular Modeling Lab, Department of Pharmaceutical Sciences and Drug Research, Punjabi university, Patiala, Punjab, India, 147002.*

[*] *E-mail: omsilakari@gmail.com, Telephone: +919501542696*

View Article Online
DOI: 10.1039/C6RA17678J

Abstract

Development of Multi-Target Directed Ligands (MTDLs) has emerged as a promising approach for targeting complex etiology of Alzheimer's disease (AD). Following this approach, a new series of 2-phenyl-1-benzopyran-4-one derivatives was designed, synthesized and biologically evaluated as inhibitors of acetylcholinesterases (AChEs), advanced glycation end products (AGEs) formation and also for their radical scavenging activity. The *in vitro* studies showed that the majority of synthesized derivatives inhibited acetylcholinesterase (AChE) with IC_{50} values in the low-micromolar range. Among them, inhibitors **7a 7h** and **7k**, strongly inhibited AChE, with IC_{50} value of 6.33, 7.56 and 11.0 nM, respectively, and were more potent than the reference compound donepezil. Moreover, the molecular docking study displayed that most potent compounds simultaneously bind to catalytic active site and peripheral anionic site of AChE. Besides, these compounds exhibited greater ability to inhibit advanced glycation end products formation with additional radical scavenging property. Thus, 2-phenyl-1-benzopyran-4-one derivatives might be the promising lead compounds as potential poly-functional anti-Alzheimer's agents.

Keywords: Alzheimer's disease, Acetylcholinesterase, Antioxidants, benzopyrans, Flavonoids, AGEs

View Article Online
DOI: 10.1039/C6RA17678J

1. Introduction

Alzheimer's disease (AD) is the most common form of irreversible dementia in the ageing patients. It is a neurodegenerative disorder associated with a selective loss of cholinergic neurons and subsequent reduction of acetylcholine (ACh) in the brain leading to progressive decline in cognitive, executive and memory functions and eventually to incapacitating dementia before death.[1,2] The prevalence of AD dramatically increases with age and it doubles for every five-year interval after the age of 65.[3] Besides several diverse hallmarks such as β-amyloid (Aβ) deposits, τ-protein aggregation and low levels of acetylcholine (ACh), AD brains display constant evidence of oxidative damage.[4-7] Cholinergic hypothesis represents one of the conventional hypothesis which proposes that the extensive decrease of ACh leads to cognitive and memory deficits in AD patients. Acetylcholinesterase (AChE) is the key enzyme, which hydrolysis acetylcholine (ACh) at the cholinergic synapses. Acetylcholinesterase inhibitors (AChEIs) could increase the level of ACh in AD patients through the inhibition AChE and, therefore, relieve some symptoms experienced by patients.[8,9] Till now, AChEIs are the only drugs used clinically for the treatment of AD (Figure 1).[10,11] Pathogenesis of AD is significantly impacted by oxidative stress which may further promotes the formation of amyloid plaques and neurofibrillary (NFT) tangles in AD.[12,13] Oxidative stress particularly induces injury in the most cellular macromolecules of AD brain including nucleic acids, proteins, and lipids. These findings support the 'oxidative stress hypotheses of AD, of which reactive oxygen species (ROS) play a key role in AD onset and progression.[14] Therefore, drugs aimed at clearing or preventing the formation of the free radicals may be useful for the management of AD.

The advanced glycation end-products (AGEs) are senescent macroprotein derivatives, formed through the non-enzymatic glycation (called the "Maillard reaction"), involved in the pathogenesis of AD.[15-17] Glycation of Aβ or tau is reported to enhance its aggregation and subsequent formation of senile plaques (SPs) and paired helical filaments in AD brain, respectively. Moreover, AGEs interact with RAGE (receptor for AGEs) that provokes the generation of ROS and vascular inflammation, and consequently alters the various gene expressions in several types of cells, which could contribute to the pathological changes of AD as well.[18-20]

View Article Online
DOI: 10.1039/C6RA17678J

The current drugs for treatment of AD are limited to mainly four AChE inhibitors. However, due to complexity of AD and involvement of various molecular pathways in its progression, modulation of single pathway, might not be sufficient to produce desire efficacy of single target therapy with AChE inhibitors.[21-24] Various approaches can be used like hybrids, chimers, mutual prodrugs, multi-target directed ligands (MTDLs), polyfunctional agents etc. for such type of complex diseases. Thus, multifactorial nature of AD demands the designing of polyfunctional agents simultaneously acting on more than one pathway rather than only one. Noticeably, drug therapy of complex diseases with polyfunctional compounds embracing diverse biological properties with single bioavailability and pharmacokinetic metabolism, will have pronounced advantage over individual-targeted drugs. In the present study, the well-established molecular pathways *i.e.* acetylcholinesterase (AChE), oxidative stress, and AGEs have been explored for the designing of polyfunctional agents for effective therapy of AD than existing one.

Selection of appropriate privileged scaffold for designing of polyfunctional drug is a crucial step in the search of clinical candidate for the treatment of AD. After critical literature review, Flavonoid or 2-phenyl-1-benzopyran-4-one as a privileged scaffold was considered for present study as it possesses a broad range of pharmacological properties such as anti-inflammatory,[25] anti-oxidative,[26] AGEs inhibitory effects,[27] and neuroprotective effects against AChE. Flavonoids or 2-phenyl-1-benzopyran-4-one are also known for their inhibition of amyloid β peptide aggregation, another key feature in AD. Aβ peptides can form insoluble plaques resulting in the formation of senile plaques and then to neurofibrillary tangles, neuronal cell death, and ultimately dementia. This privileged scaffold based single targeted molecules have previously been reported for different pathways of AD. Thus, the designing and synthesis of new polyfunctional flavonoid derivatives is an interesting strategy for the management of AD.[28,29]

Recently many studies revealed that tertiary amine at the terminal alkyl chain present in flavonoid moiety are required for adequate AChE inhibition.[30] To investigate the influence of methoxy group on B-ring, with appropriate secondary amines using two carbon spacer on ring-A of flavone, a new series of 2-phenyl-1-benzopyran-4-one derivatives were synthesized in short steps and newly synthesized derivatives were primarily evaluated for *in vitro* AChE inhibition. Additionally, *in vitro* anti-oxidative and AGEs inhibitory potential of these compounds were also determined.

View Article Online
DOI: 10.1039/C6RA17678J

2. Result and Discussion

2.1. Chemistry

First, to assess the influence of introduction of the aminoalkyl chain, compounds **7**(**a–k**), which have a -OCH_3 group at 4th position of the ring-B and various aminoalkyl moieties at the 6-position of the A-ring, were synthesized. The synthetic methodologies employed to develop intermediates (**5**) and target compounds **7(a–k)** are outlined in scheme S1 and 1, respectively. The key intermediates were prepared according to widely used Baker-venkataraman rearrangement with slight modifications.[31,32] The alkylation of **5** with α, ω-dibromoalkanes in acetone provided intermediate **6** in adequate yields. Finally, the reaction of **6** with commercially available secondary amines under reflux in acetonitrile in the presence of K_2CO_3 produced the final compounds **7(a–k)** in 50–80% yields. The compounds were dried and then, purified on silica columns using chloroform: methanol (9:1) as solvent. The structures and purities of the target compounds were confirmed by IR, ^{1}H NMR, ^{13}C NMR, mass and elemental analysis.

2.2. In vitro inhibition studies on AChE

To determine the potential of target compounds **7(a–k)** for the treatment of AD, their inhibition towards AChE (brain homogenate) was determined by the Ellman method with slight modifications using donepezil as reference compound.[33] The IC_{50} values of all tested compounds for AChE inhibition are summarized in **Table 1**. With the aim of improving the interaction of the synthesized compounds with catalytic anionic site (CAS) and peripheral anionic site (PAS) of AChE, different amines were selected and joined with 2-phenyl-1-benzopyran-4-one scaffold by a two carbon spacer exhibiting different levels of inhibitory activities against AChE. From **Table 1**, it could be seen that most of the tested compounds **7**(**a–k**) had significant AChE inhibitory activity. Compound **7h**, **7k** and **7a**, with a 4-methylpiperidine, 4-hydroxyethylpiperazine and morpholino group combined with flavonoid using a two carbon spacer are the most potent inhibitors for AChE with an IC_{50} value of 6.33, 7.56 and 11.0 nM, respectively.

The screening data exhibited that the terminal amino group of alkyl side chain at 7th position of 2-phenyl-1-benzopyran-4-one moiety significantly influenced the inhibitory activities. Compounds with different amines at two carbon spacer were compared for their ability to inhibit AChE enzyme. The unsubstituted piperazine derivative (**7c**) has moderate activity (IC_{50}=51 nM)

View Article Online
DOI: 10.1039/C6RA17678J

whereas methyl substituted piperazine (**7d**) significantly increases the activity (IC_{50}=31.0 nM). Furthermore, the introduction of hydroxyethyl group (**7k**) in piperazine increases activity with maximum IC_{50}=7.56 nM, which is superior to reference drug donepezil (IC_{50}=12.7 nM).

Ring size of terminal cyclic amine was also evaluated for its effect on AChE inhibitory activity. A general observation was extracted out that six membered cyclic amine derivatives **7a**, **7b**, **7c**, **7d**, **7h**, **7i** and **7k** (IC_{50} ranging from 6.33-51.0 nM) showed better activity than five membered cyclic amine derivatives **7e** and **7j** (IC_{50} values 104.8 and 108.3 nM). This may be due to improper fitting of five membered ring systems into the gorge of the enzyme.

Particularly 4-methylpiperidine derivative (**7h**) appears to be the most potent compound against AChE, with an IC_{50} value of 6.33 nM. Contemporarily, this compound proves to be about 2-fold more potent than donepezil and 3.5-fold more potent than unsubstituted piperidine containing compound (**7b**, IC_{50}=21.7 nM). Instead, compounds (**7c** and **7d**) possessing additional nitrogen atom in the terminal group, exhibited low potency than the compound having only one nitrogen atom (**7b** and **7h**). Moreover, morpholino derivative (**7a**) with IC_{50} value of 11.0 nM, also feature good inhibitory activity against AChE. The diethyl amino derivative (**7f**) with IC_{50} value of 27.0 nM is about 3-fold more potent than dimethyl amino derivative (**7g**, IC_{50}=77.4 nM). Interestingly, the diethylamine and dimethylamine derivatives are less effective than morpholino and piperazine derivatives. Graph showing the comparison of AChE inhibitory potencies of synthesized derivatives is displayed in Figure S2.

2.3. In vitro antioxidant activity

Oxidative stress plays an important role in neuronal degeneration in AD. Its reduction is another decisive aspect in designing poly-functional agents for AD treatment. Synthesized compounds **7(a–k)** were tested for their free radical scavenging activities using 1,1-diphenyl-2-picryl-hydrazyl (DPPH) assay at 517nm. The DPPH scavenging activities of test compounds are summarized in Table 1 and displayed in Figure S2. Results clearly indicate that almost all compounds exhibited radical scavenging activity, among these **7c**, **7h**, **7i** & **7k** are comparable to ascorbic acid. The compound **7k** was found to be the best radical scavenger (EC_{50}=21.5 nM). This might be due to radical scavenging property of hydroxyl group. Compounds **7h** and **7c** with EC_{50} values 24.6 and 30.5, respectively also show good radical scavenging activity. The positive

View Article Online
DOI: 10.1039/C6RA17678J

charge of free –NH groups intensify the free radical quenching. The flavonoid moiety due to conjugation system appears to be crucial to the compound's radical scavenging ability. It might be attributed to the presence of electron rich benzopyran or flavone nucleus that can stabilize the free radicals via resonance effect. The compounds **7d**, **7b**, **7f** and **7a** exhibited moderate activity with EC_{50} values range from 45.4 to 54.3 nM.

2.4. Advanced glycation end-product formation inhibitory activity

All the synthesized compounds **7(a–k)** were subjected to *in vitro* bioassay of AGEs formation inhibitory activity using method reported by Matsuura *et al* with slight modification.[34] The potential of the compounds **7(a–k)** to inhibit AGEs-formation is summarized in Table 1 and displayed in Figure S3. All the synthesized compounds showed considerable AGEs formation inhibitory activity as the fluorescence of AGEs was shown to be significantly inhibited by the all the synthesized compounds. Among the various synthesized compounds, the compound **7k** (IC_{50}=36.0 μM) was found to be significantly potent than the reference drug aminoguanidine (IC_{50}=40.5 μM). The compounds **7f**, **7h**, **7d** and **7a** (IC_{50} value ranging from 43.5 to 56.3 μM) exhibited moderate inhibitory activity as compared to the standard drug. However, the compounds **7b**, **7i**, **7c**, **7g**, **7e** and **7j** exhibited lower anti-glycating activity than the standard drug (IC_{50} value ranging from 64.0 to 113.1 μM). As evident from the results, among all the synthesized compounds, the compounds with hydroxyl substitution (**7k**) was found to be more active than the derivatives that lack hydroxyl group. The compound with 4-methylpiperidine moiety (**7h**) exhibited good anti-glycating activity than the compound with no substitution on piperidine (**7b**). The six membered cyclic amines (**7k**, **7h**, **7d**, **7a**, **7b** and **7c**) have good to moderate anti-glycating activity as compared to five membered cyclic amines (**7e** and **7j**). The flavonoid with diethyl amine moiety (**7f**, IC_{50}=50.3 μM) exhibited good activity than dimethylamine (**7g**, IC_{50}=72.2 μM).

2.5. Kinetic characterization of AChE inhibition

Based on the *in vitro* results of AChE inhibition, kinetic study was carried out on most potent inhibitor **7h** to investigate the type of enzyme inhibition. The Lineweaver–Burk plots (Figure 2) displayed both increased slopes (decreased V_{max}) and intercepts (higher K_m) at higher concentration of the inhibitor **7h**, indicating a mixed-type inhibition. Thus, compound **7h** might

View Article Online
DOI: 10.1039/C6RA17678J

be able to bind with both catalytic anionic site (CAS) as well as peripheral anionic site (PAS) of AChE.

2.6. Molecular docking studies

In order to explore the binding patterns of 2-phenyl-1-benzopyran-4-one derivatives in active site of AChE, molecular docking studies were carried out for two most potent inhibitors **7h** and **7k**. Molecular docking study was carried out with the available crystal structure of Torpedo californica AChE (TcAChE) (1EVE). The 3D structure of TcAChE enzyme revealed that the active site is located at the bottom of a deep and narrow gorge comprising Trp84 and Phe330 residues in the CAS. Additionally, PAS is present near the active site gorge mainly comprising of aromatic residues Tyr121, Tyr70, Trp279, Tyr334 and Asp72.[35] These compounds showed nice fit in the active site by interacting with both catalytic site and peripheral anionic site of the enzyme simultaneously to provide maximal inhibitory profile. The position of compound **7h** and **7k** with respect to the key residues in the binding site is shown in Figure 3.

As shown in Figure 3, the compound **7h** binds along the active-site gorge, extending from the anionic subsite near Trp84 to the peripheral anionic site (PAS) near Trp279. The compound **7h** displayed π-π stacking with conserved amino acid residue Trp279, a major component of a peripheral "anionic" site (PAS). The quaternary amine of 4-methylpiperidine moiety showed π-cationic interactions with an aromatic residue, Phe330, a residue of hydrophobic site, and with Tyr334 and Asp72 amino acid residue of PAS, 14 Å from the active site, near the top of the gorge. It also showed one hydrogen bond between carbonyl oxygen of the ring C and Arg289, acyl binding pocket. On the other hand, compound **7k** showed π-π stacking of ring-A and ring-B with Phe331, acyl binding pocket and Trp279 amino acid residue of peripheral anionic site, respectively. It also interacts with Phe288 and Arg289 amino acids, acyl binding pocket residue of catalytic triad via hydrogen bonding. The hydroxyl oxygen of piperazine moiety forms hydrogen bond with hydroxyl hydrogen of Tyr130 and Glu199, choline binding site (Figure 3). The result of docking study revealed that the dual binding profile of selected compounds was found due to hydrogen bond, π–π (aromatic) and hydrophobic interactions with both CAS and PAS of AChE. Further, MM-GBSA binding energies, summarized in Table S1, were calculated for all the synthesized compounds to estimate relative binding affinity.

View Article Online
DOI: 10.1039/C6RA17678J

2.7. ADMET prediction

To predict the drug-likeness of the designed compounds, a few indicators of their pharmacokinetic profile like Lipinski's parameters, QPlogPo/w, Polar Surface Area (PSA), QPlogKhsa, QPPCaco, QPlogBB, QPLogKhsa, QPlogBB, QPPMDCK etc were predicted using QikProp, v. 3.5 (Table S1).[36] The important physiochemical features of CNS drugs are mostly associated to their ability to cross the blood–brain barrier (BBB) and subsequent CNS activity. The results showed that compounds **7(a–k)** obey Lipinski's rule of five (mol_MW <500, QPlogPo/w <5, donorHB≤5, accptHB≤10) and therefore are drug like molecules. Based on the predicted values for QPlogBB and CNS activity, all compounds might be able to penetrate into the CNS. PSA is another important predictor for ability to cross Blood Brain Barrier (BBB). For a compound to be CNS active, PSA should be lower and the value should range from 50 to 70 Å.[37] The QPlogKhsa prediction value revealed about the protein binding amount of CNS active drugs which is also a vital consideration and tends to be rather high. The predicted values of QPlogKhsa for all compounds **7(a-k)** showed their strong binding with plasma protein. All the synthesized compounds PSA values are within acceptable limit that support their ability to infiltrate the BBB. Among calculated parameters, QPPCaco, QPlogBB, QPLogKhsa, and QPPMDCK primarily intemperate the capability of the compound's distribution inside the body. Most of the compounds exhibited moderate to significant penetrability for both *in vitro* MDCK cells and *in vitro* Caco-2 cells except compound **7c**. Furthermore, all compounds exhibited good to significant oral absorption. The predicted ADME properties revealed that all compounds **7(a-k)**, have drug-like properties and could be considered as good drug candidate.

2.8. Determination of brain AChE activity

Anti-Alzheimer drug must be able to cross the blood brain barrier (BBB) efficiently and enter into the brain. Thus, to determine whether the most active compound **7h** as a representative could penetrate the BBB, the brain AChE activity was measured as an indirect method.[38,39] Various concentrations of **7h** (50, 100 and 200 mg/kg) was administered via intraperitoneal injection to the mice (25-30 g). After 48 h of administration, mice were sacrificed and brain homogenates were prepared. To determine the brain AChE activity, supernatant of brain homogenate was used. The rate of hydrolysis of acetylthiocholine (ATCh) (15 µL of 1 mM) by brain AChE at 10, 20, 30, 40 and 50 µL was measured using Ellman method.[33] The rate of hydrolysis of ATCh by brain AChE was

View Article Online
DOI: 10.1039/C6RA17678J

decreaseed with increase in administered dose of **7h**. Therefore, after treatment with **7h**, the brain AChE activity was decrease in dose dependent manner which is possible only if **7h** had penetrated the BBB and inhibit brain AChE activity (Figure S4).

2.9. Molecular Dynamic Simulations

Molecular dynamic simulations (MD) were undertaken to study protein-ligand interactions in dynamic motion contributing for their thermodynamic stability and to visualize the effect of ligand binding induced conformational changes at AChE pocket. The protein ligand binding complex of AChE and most active compound **7h** was used for MD simulations. The important interactions after MD simulations were conserved although a slightly different interaction pattern was observed. After MD, compound **7h** displayed strong hydrogen bonding with Asp72, Phe288 and Arg289. Compound **7h** also showed hydrophobic interactions and π-π stacking interactions with Tyr334 and Trp279 respectively (Figure 4). These interactions can be categorized by type and summarized, as shown in the protein-ligand contacts plot (Figure S5). After MD simulations, the Root mean square deviation (RMSD) was calculated for the trajectory of complex and plotted against time (ns). The RMSD plot showed that the docked complex was quite stable throughout with minor fluctuations in the range of 1–1.6 Å. Higher stability was observed from 2 to 5 ns (Figure S5) and the stability of the simulated system indicate the inhibitory nature of the **7h** on AChE.

3. Conclusion

In the present study, a new series of 2-phenyl-1-benzopyran-4-one derivatives have been developed as potential poly-functional anti-Alzheimer's agents. These compounds were evaluated *in vitro* and *in silico* against important biological targets and molecular processes including AChE enzyme, AGEs formation with free radical scavenging activity. Among the synthesized compounds most of the compounds showed the AChE inhibitory activity with good radical scavenging and AGEs product formation inhibitory activity. The structure activity relationship studies revealed that the extent of AChE inhibition was mainly influenced by the presence of the electron releasing group on ring-C and substituted cyclic amine on ring-A of flavonoid moiety via two carbon spacer. The compounds **7h** and **7k** (IC_{50} = 6.33 nM and 7.53 nM, respectively) displayed about 2- and 1.5-fold higher potency for AChE than reference

View Article Online
DOI: 10.1039/C6RA17678J

compound donepezil. Moreover, the *in silico* pharmacokinetic profiles were predicted and revealed that all compounds have drug-like properties with good penetration in brain and good oral absorption. Further investigation of molecular modeling study indicated that compound **7h** and **7k** simultaneously bind with both CAS and PAS of active site gorge. Additionally, these compounds had significant capacity to absorb free radicals and inhibit the AGEs product formation. The synthesized 2-phenyl-1-benzopyran-4-one derivatives **7h** and **7k** have been found to be maximally potent poly-functional molecules. This poly-functional attribute, make them potential candidates for the development of drugs for Alzheimer's disease. In summary, these preliminary findings suggested that designed new compounds could be further investigated for pharmacological development in AD therapy.

4. Experimental Section

4.1. Chemistry

All chemicals and solvents required for synthesis were procured commercially from various suppliers and were of LR grade, used without any purification. The solvents were dehydrated according to standard methods. The synthesis was carried out using magnetic stirrer and hot plate (Perfit), and solvents were recovered using rotary vacuum evaporator (Perfit). The completion of each reaction was monitored by thin layer chromatography (DC-Alufolien (20x20 cm) Kieselgel 60 F_{254} chromato plates) using hexane:ethylacetate (6:4, *v/v*) and chloroform:methanol (9:1 *v/v*) as a TLC development solvent system. Impure compounds and intermediates were purified on silica columns from appropriate solvent. The melting points were recorded on an electronic melting point apparatus. The purity of all organic compounds was confirmed by TLC, IR, ^{1}H NMR, ^{13}C NMR and Mass spectroscopy. IR spectra were recorded on a Bruker (Alpha E) FT/IR spectrophotometer, ^{1}H-NMR spectra were recorded on a Bruker Advance II 400 MHz NMR spectrometer using chloroform ($CDCl_3$) or dimethylsulfoxide (DMSO-d_6) as solvent. The chemical shifts are reported in parts per million (δ) downfield from TMS and coupling constants are reported in hertz (Hz). Proton coupling patterns are abbreviated as single (s), double (d), triplet (t) and multiple (m). Mass spectra (ESI-MS) were recorded with a Waters, Q-TOF Micromass (LC-MS).

*4.1.1. General procedures for the synthesis of intermediate o-Benzoyloxyacetophenone (**3**)*

View Article Online
DOI: 10.1039/C6RA17678J

At first, the substituted *o*-benzoyloxyacetophenone (**3**) was synthesized by stirring the mixture of substituted *o*-hydroxyacetophenone (0.1mol) and substituted benzoyl chloride (0.15mol) in dry pyridine. During the reaction, the mixture evolved spontaneous heat, and after about 15 minutes when the temperature comes down to room temperature, the mixture was poured, with constant stirring, into 3% hydrochloric acid containing crushed ice resulting in the precipitation of solid residue. The solid residue was then filtered and washed with methanol followed by water. The filtered residue was air dried, and re-crystallized from methanol resulting in the white precipitates of substituted *o*-benzoyloxyacetophenone, yield 90%.

*4.1.2. General procedures for the synthesis of intermediate o-Hydroxydibenzoylmethane (**4**)*

To a warm solution of substituted *o*-benzoyloxyacetophenone (**3**) in dry pyridine, hot pulverized 85% potassium hydroxide was added followed by mechanical stirring for 30 minutes resulting in the gradual appearance of yellowish brown precipitates of potassium salt of substituted *o*-hydroxydibenzoylmethane (**4**). The reaction mixture was brought down to room temperature, and subsequently acidified with 10% acetic acid to desalt the compounds. The light-yellow precipitates of diketone (**4**) were filtered and dried, yield 85%.

*4.1.3. General procedures for the synthesis of intermediate 7-hydroxy-2-(4-methoxyphenyl)-4H-chromen-4-one (**5**)*

The substituted *o*-hydroxydibenzoylmethane (**4**), in the presence of glacial acetic acid and conc. sulphuric acid, was refluxed on water bath for 1h, to achieve the cyclized product. Then, the reaction mixture was poured onto crushed ice with vigorous stirring resulting in the precipitation of the7-hydroxy-2-(4-methoxyphenyl)-4*H*-chromen-4-one (**5**). The product was filtered, thoroughly washed with water to make it free from acid and dried. Then, purified on silica columns using hexane: ethyl acetate (6:4%) as solvent. (Scheme S1)

*4.1.4. General procedures for the synthesis of intermediate 7-(2-bromoethoxy)-2-(4-methoxyphenyl)-4H-chromen-4-one (**6**)*

The synthetic protocol for intermediate 7-(2-bromoethoxy)-2-(4-methoxyphenyl)-4*H*-chromen-4-one (**6**) is outlined in Scheme 1. Anhydrous K_2CO_3 (10.0 mmol) and α,ω-dibromoalkane (4.0 mmol) were added to a solution of intermediate **5** (2.0 mmol) in acetone. After reflux for 10h until the starting material **5** disappeared, the solvent was removed under vacuum; the residue was

View Article Online
DOI: 10.1039/C6RA17678J

poured into water and extracted with EtOAc, the solution was dried over Na_2SO_4 and then concentrated. Then, the intermediate **6** was purified on silica columns using $CHCl_3$:MeOH (9:1%) as solvent.[40]

*4.1.4. General procedures for the synthesis of final compounds **7(a-k)**.*

To a solution of intermediate **6** (0.5 mmol) in CH_3CN (10 mL) was added different amines (1.0 mmol) and anhydrous K_2CO_3 (2.5 mmol). After stirring at 60°C for 12 h, the solvent was removed under vacuum, the mixture was diluted with $CHCl_3$ and then washed with water and brine. The organic layer was dried over Na_2SO_4, filtered, concentrated in vacuo, and the compounds **7(a-k)** were purified by column chromatography with $CHCl_3$:MeOH (95:5%) elution.[40] (Scheme 1)

*7-hydroxy-2-(4-methoxyphenyl)-4H-chromen-4-one (**5**):*

Brown black, amorphous solid, yield 91%, m.p.: 231-236°C; ^{1}H-NMR (400 MHz, DMSO-d_6, δ ppm): 3.87 (3H, s, -CH_3), 6.69 (1H, s), 6.87-6.90 (1H, dd, *J*= 2.20, 8.68 Hz, *ArH*), 6.94 (1H, d, *J*= 2.16 Hz, *ArH*), 7.05-7.08 (2H, d, *J*= 2.96 Hz, *ArH*), 7.89 (1H, d, *J*= 8.68 Hz, *ArH*), 7.94-7.96 (2H, dd, *J*= 1.88, 7.0 Hz, *ArH*), 10.62 (1H, s, -*OH*). IR: (C=O) 1652 cm^{-1} (s) (O-H) 3701 cm^{-1}, MS (ESI) m/z = 269.1 $[M+H]^+$. Elemental Anal. Calcd for $C_{16}H_{12}O_4$: C, 71.64; H, 4.51. Found: C, 71.51; H, 4.82; R_f Value: 0.53 (Hexane: Ethyl acetate, 6:4).

*7-(2-bromoethoxy)-2-(4-methoxyphenyl)-4H-chromen-4-one **(6):***

Light Yellow, Amorphous, yield 60%; ^{1}H-NMR (400 MHz, $CDCl_3$, δ ppm): 8.14-8.16 (1H, d, *J* = 8.72 Hz, *ArH*), 7.85-7.87 (2H, dd, *J* = 6.88 Hz, *ArH*), 6.97-7.03 (4H, m, *ArH*), 6.69 (1H, s, *ArH*), 4.40-4.43 (2H, t, *J* = 6.28 Hz, -CH_2) 3.89 (3H, s, -OCH_3) 3.69-3.72 (2H, t, *J* = 6.28 Hz, -CH_2). Anal. Calcd for $C_{18}H_{15}BrO_4$: C, 57.62; H, 4.03. Found: C, 58.51; H, 5.31; R_f Value: 0.65 ($CHCl_3$: MeOH, 9:1).

*2-(4-methoxyphenyl)-7-(2-morpholinoethoxy)-4H-chromen-4-one (**7a**):*

Intermediate **6** was treated with morpholine according to general procedure to give the desired product **7a** as light yellow, solid crystalline, yield 65%; IR (KBr) (cm^{-1}): 1650 cm^{-1} (C=O, str, s), 1605 cm^{-1} (C=C, s), 1263 cm^{-1} (C-O, asym., s), 1373 cm^{-1} (C-N, str, s); ^{1}H-NMR (400 MHz,

View Article Online
DOI: 10.1039/C6RA17678J

$CDCl_3$, δ ppm): 8.11-8.13 (1H, d, *J* = 8.68 Hz, *ArH*), 7.84-7.87 (2H, dd, *J* = 6.84, 2.08 Hz, *ArH*), 6.96-7.03 (4H, m, *ArH*), 6.68 (1H, s, *ArH*), 4.21-4.24 (2H, t, *J* = 5.60 Hz, -CH_2) 3.89 (3H, s, -OCH_3) 3.74-3.76 (4H, t, *J* = 4.72 Hz, -CH_2) 2.85-2.88 (2H, t, *J* = 5.72 Hz, -CH_2) 2.59-2.62 (4H, t, *J* = 5.72 Hz, -CH_2); ^{13}C NMR (100 MHz, $CDCl_3$): 177.84, 163.10, 162.28, 157.83, 127.85, 127.07, 124.13, 117.93, 114.47, 114.45, 106.14, 101.12, 66.92, 66.53, 57.35, 55.52, 54.13; MS (ESI) m/z = 382.31 $[M+H]^+$. Anal. Calcd for $C_{22}H_{23}NO_5$: C, 69.28; H, 6.08; N, 3.67. Found: C, 69.21; H, 5.95; N, 3.26; R_f Value: 0.30 ($CHCl_3$: MeOH, 9:1).

*2-(4-methoxyphenyl)-7-(2-(piperidin-1-yl)ethoxy)-4H-chromen-4-one (**7b**):*

Intermediate **6** was treated with piperidine according to general procedure to give the desired product **7b** as light yellow, solid amorphous, yield 60%; IR (KBr) (cm^{-1}): 1630 cm^{-1} (C=O, str, s), 1601 cm^{-1} (C=C, s), 1258 cm^{-1} (C-O, asym., s), 1359 cm^{-1} (C-N, str, s); ^{1}H-NMR (400 MHz, $CDCl_3$, δ ppm): 8.10-8.12 (1H, d, *J* = 8.64 Hz, *ArH*), 7.84-7.87 (2H, dd, *J* = 7.00, 1.88 Hz, *ArH*), 7.00-7.03 (2H, dd, *J* = 7.08, 1.80 Hz, *ArH*), 6.98-6.99 (1H, d, *J* = 2.36 Hz, *ArH*), 6.96 (1H, s, *ArH*), 6.68 (1H, s, *ArH*), 4.21-4.24 (2H, t, *J* = 5.92 Hz, -CH_2) 3.89 (3H, s, -OCH_3) 2.84-2.87 (2H, t, *J* = 5.92 Hz, -CH_2), 2.56 (2H, m, -CH_2) 1.61-1.66 (4H, m, -CH_2) 1.45-1.48 (2H, m, -CH_2); ^{13}C NMR (100 MHz, $CDCl_3$): 177.86, 163.20, 163.07, 162.25, 157.84, 127.85, 126.91, 124.12, 117.82, 114.60, 114.43, 106.08, 101.06, 66.57, 57.52, 55.50, 55.02, 29.70, 29.37, 25.76; MS (ESI) m/z = 380.20 $[M+H]^+$. Anal. Calcd for $C_{23}H_{25}NO_4$: C, 72.80; H, 6.64; N, 3.69. Found: C, 72.29; H, 7.47; N, 3.48; R_f Value: 0.35 ($CHCl_3$: MeOH, 9:1).

*2-(4-methoxyphenyl)-7-(2-(piperazin-1-yl)ethoxy)-4H-chromen-4-one (**7c**):*

Intermediate **6** was treated with piperazine according to general procedure to give the desired product **7c** as light yellow, solid amorphous, yield 55%; IR (KBr) (cm^{-1}): 1651 cm^{-1} (C=O, str, s), 1606 cm^{-1} (C=C, s), 1263 cm^{-1} (C-O, asym., s), 1374 cm^{-1} (C-N, str, s); ^{1}H-NMR (400 MHz, DMSO-d_6, δ ppm): 8.00-8.02 (2H, d, *J* = 8.88 Hz, *ArH*), 7.92-7.94 (1H, d, *J* = 8.80 Hz, *ArH*), 7.25-7.26 (1H, d, *J* = 2.28 Hz, *ArH*), 7.08-7.10 (2H, d, *J* = 8.88 Hz, *ArH*), 7.00-7.03 (1H, dd, *J* = 8.80, 2.28 Hz, *ArH*), 6.79 (1H, s, *ArH*), 4.22-4.25 (2H, t, *J* = 5.64 Hz, -CH_2) 3.87 (3H, s, -OCH_3) 2.75-2.81 (5H, m, -CH_2, -*NH*), 2.52-2.53 (6H, t, *J* = 1.64 Hz, -CH_2); ^{13}C NMR (100 MHz, $CDCl_3$): 177.87, 163.10, 162.28, 157.88, 127.86, 127.05, 124.09, 117.89, 114.50, 114.44, 106.09, 101.11, 66.52, 57.27, 55.51, 53.81, 45.29; MS (ESI) m/z = 381.34 $[M+H]^+$. Anal. Calcd

View Article Online
DOI: 10.1039/C6RA17678J

for $C_{22}H_{24}N_2O_4$: C, 69.46; H, 6.36; N, 7.36. Found: C, 69.11; H, 6.92; N, 7.49; R_f Value: 0.25 ($CHCl_3$: MeOH, 9:1).

*2-(4-methoxyphenyl)-7-(2-(4-methylpiperazin-1-yl)ethoxy)-4H-chromen-4-one (**7d**):*

Intermediate **6** was treated with 4-methylpiperazine according to general procedure to give the desired product **7d** as brown black, solid amorphous flakes, yield 78%, mp 231-236°C; IR (KBr) (cm^{-1}): 1652 cm^{-1} (C=O, str, s), 1610 cm^{-1} (C=C, s), 1258 cm^{-1} (C-O, asym., s), 1370 cm^{-1} (C-N, str, s); ^{1}H-NMR (400 MHz, $CDCl_3$, δ ppm): 8.10-8.12 (1H, d, *J* = 8.64 Hz, *ArH*), 7.85-7.87 (2H, dd, *J* = 6.8, 2.08 Hz, *ArH*), 7.01-7.03 (2H, m, ArH), 6.96-7.03 (2H, dd, *J* = 10.84, 1.84, *ArH*), 6.68 (1H, s, *ArH*), 4.20-4.23 (2H, t, *J* = 6.00 Hz, -CH_2) 3.89 (3H, s, -OCH_3) 2.83-2.86 (2H, t, *J* = 6.00 Hz, -CH_2), 2.09-2.15 (2H, m, -CH_2) 1.64-1.69 (6H, m, -CH_2) 1.25-1.30 (3H, m, -OCH_3); ^{13}C NMR (100 MHz, $CDCl_3$): 177.94, 163.35, 163.11, 162.25, 157.91, 127.91, 127.01, 124.21, 117.85, 114.68, 114.49, 106.15, 101.12, 66.89, 57.33, 55.56, 54.63, 30.62; MS (ESI) m/z = 432.25 $[M+K]^+$. Anal. Calcd for $C_{23}H_{26}N_2O_4$: C, 70.03; H, 6.64; N, 7.10. Found: C, 70.45; H, 6.80; N, 6.91; R_f Value: 0.36 ($CHCl_3$: MeOH, 9:1).

*2-(4-methoxyphenyl)-7-(2-(pyrrolidin-1-yl)ethoxy)-4H-chromen-4-one (**7e**):*

Intermediate **6** was treated with pyrrolidine according to general procedure to give the desired product **7e** as light brownish, solid amorphous, yield 50%; %; IR (KBr) (cm^{-1}): 1627 cm^{-1} (C=O, str, s), 1602 cm^{-1} (C=C, s), 1258 cm^{-1} (C-O, asym., s), 1360 cm^{-1} (C-N, str, s); ^{1}H-NMR (400 MHz, DMSO-d_6, δ ppm): 8.10-8.12 (1H, d, *J* = 8.76 Hz, *ArH*), 7.84-7.88 (2H, m, *ArH*), 6.96-7.03 (4H, m, *ArH*), 6.68 (1H, s, *ArH*), 4.21-4.24 (2H, t, *J* = 5.80 Hz, -CH_2) 3.89 (3H, s, -OCH_3) 2.96-2.99 (2H, t, *J* = 5.84 Hz, -CH_2), 2.65-2.68 (4H, m, -CH_2) 1.81-1.86 (4H, m, -CH_2); ^{13}C NMR (100 MHz, $CDCl_3$): 177.94, 163.27, 163.10, 157.86, 127.88126.99, 124.14, 117.81, 114.63, 114.43, 106.10, 101.02, 67.74, 55.52, 54.76, 54.73, 23.50; MS (ESI) m/z = 366.30 $[M+H]^+$. Anal. Calcd for $C_{22}H_{23}NO_4$: C, 72.31; H, 6.34; N, 3.83. Found: C, 72.84; H, 5.67; N, 3.22; R_f Value: 0.32 ($CHCl_3$: MeOH, 9:1).

*7-(2-(diethylamino)ethoxy)-2-(4-methoxyphenyl)-4H-chromen-4-one (**7f**):*

Intermediate **6** was treated with diethylamino according to general procedure to give the desired product **7f** as light yellow, solid amorphous flakes, yield 55%; IR (KBr) (cm^{-1}): 1627 cm^{-1}

View Article Online
DOI: 10.1039/C6RA17678J

(C=O, str, s), 1597 cm^{-1} (C=C, s), 1246 cm^{-1} (C-O, asym., s), 1363 cm^{-1} (C-N, str, s); ^{1}H-NMR (400 MHz, $CDCl_3$, δ ppm): 8.10-8.13 (1H, d, *J* = 8.56 Hz, *ArH*), 7.85-7.86 (2H, dd, *J* = 6.92, 1.96 Hz, *ArH*), 7.01-7.03 (2H, m, *ArH*), 6.99.-7.00 (1H, d, *J* = 2.32 Hz, *ArH*), 6.97 (1H, s, *ArH*), 6.68 (1H, s, *ArH*), 4.16-4.19 (2H, t, *J* = 6.04 Hz, -CH_2) 3.89 (3H, s, -OCH_3) 2.94-2.97 (2H, t, *J* = 6.04 Hz, -CH_2), 2.66-2.71 (4H, q, -CH_2), 1.09-1.12 (6H, t, *J* = 7.16 Hz, -CH_3); ^{13}C NMR (100 MHz, $CDCl_3$): 177.89, 163.32, 163.07, 162.26, 157.88, 127.86, 127.00, 124.20, 117.83, 114.58, 114.45, 106.15, 101.04, 67.36, 55.51, 51.52, 47.92, 11.83; MS (ESI) m/z = 368.34 $[M+H]^+$. Anal. Calcd for $C_{22}H_{25}NO_4$: C, 71.91; H, 6.86; N, 3.81. Found: C, 71.50; H, 6.54; N, 3.50; R_f Value: 0.28 ($CHCl_3$: MeOH, 9:1).

*7-(2-(dimethylamino)ethoxy)-2-(4-methoxyphenyl)-4H-chromen-4-one (**7g**):*

Intermediate **6** was treated with dimethylamino according to general procedure to give the desired product **7g** as light yellowish brown, solid amorphous flakes, yield 60%; IR (KBr) (cm^{-1}): 1637 cm^{-1} (C=O, str, s), 1596 cm^{-1} (C=C, s), 1252 cm^{-1} (C-O, asym., s), 1361 cm^{-1} (C-N, str, s); ^{1}H-NMR (400 MHz, $CDCl_3$, δ ppm): 8.11-8.13 (1H, d, *J* = 8.60 Hz, *ArH*), 7.85-7.87 (2H, dd, *J* = 6.88, 2.04 Hz, *ArH*), 6.97.-7.03 (4H, m, *ArH*), 6.68 (1H, s, *ArH*), 4.18-4.21 (2H, t, *J* = 5.56 Hz, -CH_2) 3.89 (3H, s, -OCH_3) 2.82-2.84 (2H, t, *J* = 5.60 Hz, -CH_2), 2.39 (6H, s, -CH_3); ^{13}C NMR (100 MHz, $CDCl_3$): 177.89, 163.18, 163.08, 162.25, 127.87, 127.01, 124.12, 117.87, 114.59, 106.11, 101.02, 66.54, 57.90, 55.52, 45.82; MS (ESI) m/z = 340.34 $[M+H]^+$. Anal. Calcd for $C_{20}H_{21}NO_4$: C, 70.78; H, 6.24; N, 4.13. Found: C, 70.50; H, 6.50; N, 3.43; R_f Value: 0.24 ($CHCl_3$: MeOH, 9:1).

*2-(4-methoxyphenyl)-7-(2-(4-methylpiperidin-1-yl)ethoxy)-4H-chromen-4-one (**7h**):*

Intermediate **6** was treated with 4-methylpiperidine according to general procedure to give the desired product **7h** as brownish black, solid amorphous sticky, yield 40%; IR (KBr) (cm^{-1}): 1632 cm^{-1} (C=O, str, s), 1362 cm^{-1} (C-N, str, s); ^{1}H-NMR (400 MHz, $CDCl_3$, δ ppm): 8.10-8.12 (1H, dd, *J* = 6.80, 2.72 Hz, *ArH*), 7.86-7.84 (2H, d, *J* = 8.8 Hz, *ArH*), 7.02 (1H, s, *ArH*), 7.00 (1H, s, *ArH*), 6.98-6.96 (2H, m, *ArH*) 6.68 (1H, s, *ArH*), 4.27-4.24 (2H, t, *J* = 5.76 Hz, -CH_2), 3.89 (3H, s, -OCH_3) 2.92-2.89 (2H, t, *J* = 5.76 Hz, -CH_2), 1.25-1.42 (8H, m, -CH_2), 0.95-0.94 (3H, d, *J* = 6.0 Hz, -CH_2), 0.92-0.86 (1H, q, -CH_2); ^{13}C NMR (100 MHz, $CDCl_3$): 177.91, 163.14, 163.00, 162.27, 157.84, 127.88, 127.01, 124.07, 117.89, 114.61, 114.44, 106.07, 101.08, 66.29, 57.03,

View Article Online
DOI: 10.1039/C6RA17678J

55.52, 52.40, 33.69, 30.29, 29.72, 29.38, 21.73; MS (ESI) m/z = 394.26 $[M+H]^+$. Anal. Calcd for $C_{24}H_{27}NO_4$: C, 73.26; H, 6.92; N, 3.56. Found: C, 72.68; H, 7.26; N, 3.53; R_f Value: 0.12 ($CHCl_3$: MeOH, 9:1).

*7-(2-(benzyl(methyl)amino)ethoxy)-2-(4-methoxyphenyl)-4H-chromen-4-one (**7i**):*

Intermediate **6** was treated with N-benzylmethylamino according to general procedure to give the desired product **7i** as greyish brown, solid amorphous, yield 55%; IR (KBr) (cm^{-1}): 1624 cm^{-1} (C=O, str, s), 1595 cm^{-1} (C=C, s), 1252 cm^{-1} (C-O, asym., s), 1355 cm^{-1} (C-N, str, s); ^{1}H-NMR (400 MHz, DMSO-d_6, δ ppm): 7.99-7.97 (2H, dd, *J* = 7.0, 1.96 Hz, *ArH*), 7.95-7.93 (1H, d, *J* = 8.84 Hz, *ArH*), 7.34-7.29 (4H, m, *ArH*), 7.23 (1H, s, *ArH*), 7.19-7.18 (1H, d, *J* = 11.12 Hz, *ArH*) 7.08 (1H, d, *J* = 1.96 Hz, *ArH*), 7.06 (1H, s, *ArH*), 6.98-7.01 (1H, dd, *J* = 8.8, 2.32 Hz, *ArH*), 6.75 (1H, s, *ArH*), 4.27-4.24 (2H, t, *J* = 5.76 Hz, -CH_2), 3.87 (3H, s, -OCH_3) 3.62 (2H, s, -CH_2), 2.86-2.83 (2H, t, *J* = 5.76, 5.64 Hz, -CH_2), 2.31 (3H, m, -CH_3); ^{13}C NMR (100 MHz, $CDCl_3$): 177.95, 163.21, 163.16, 162.33, 157.91, 129.26, 128.48, 127.93, 127.47, 127.07, 124.20, 117.92, 114.62, 114.50, 106.17, 101.11, 66.90, 62.67, 55.58, 55.37, 42.93; MS (ESI) m/z = 416.34 $[M+H]^+$. Anal. Calcd for $C_{26}H_{25}NO_4$: C, 75.16; H, 6.06; N, 3.37. Found: C, 75.06; H, 6.49; N, 2.62; R_f Value: 0.20 ($CHCl_3$: MeOH, 9:1).

*7-(2-(1H-imidazol-1-yl)ethoxy)-2-(4-methoxyphenyl)-4H-chromen-4-one (**7j**):*

Intermediate **6** was treated with 4-imidazoline according to general procedure to give the desired product **7j** as light yellowish, solid amorphous powder, yield 65%; IR (KBr) (cm^{-1}): 1625 cm^{-1} (C=O, str, s), 1598 cm^{-1} (C=C, s), 1256 cm^{-1} (C-O, asym., s), 1367 cm^{-1} (C-N, str, s); ^{1}H-NMR (400 MHz, $CDCl_3$, δ ppm): 8.13-8.11 (1H, d, *J* = 8.6 Hz, *ArH*), 7.84-7.82 (2H, d, *J* = 8.88 Hz, *ArH*), 7.63 (1H, s, *ArH*), 7.10 (1H, s, *ArH*), 7.07 (1H, s, *ArH*), 7.02-7.00 (2H, d, *J* = 8.88 Hz, *ArH*), 6.96-6.95 (1H, d, , *J* = 2.24 Hz, *ArH*), 6.94-6.91 (1H, m, *ArH*), 6.67 (1H, s, *ArH*), 4.43-4.40 (2H, t, *J* = 4.84 Hz, -CH_2), 4.34-4.32 (2H, t, *J* = 5.04 Hz -CH_2), 3.88 (3H, s, -OCH_3); ^{13}C NMR (100 MHz, $CDCl_3$): 177.73, 163.24, 162.34, 162.14, 157.65, 129.81, 127.88, 127.37, 123.91, 118.42, 114.46, 113.97, 106.11, 101.41, 67.71, 55.53, 46.22; MS (ESI) m/z = 363.38 $[M+H]^+$, 385.35 $[M+Na]^+$. Anal. Calcd for $C_{21}H_{18}N_2O_4$: C, 69.60; H, 5.01; N, 7.73. Found: C, 69.83; H, 5.44; N, 7.51; R_f Value: 0.20 ($CHCl_3$: MeOH, 9:1).

*7-(2-(4-(hydroxyethyl)piperazin-1-yl)ethoxy)-2-(4-methoxyphenyl)-4H-chromen-4-one (**7k**):*

View Article Online
DOI: 10.1039/C6RA17678J

Intermediate **6** was treated with 4-hydroxymethylpiperazine according to general procedure to give the desired product **7k** as dark brown, solid amorphous, yield 45%; IR (KBr) (cm^{-1}): 1630 cm^{-1} (C=O, str, s), 1365 cm^{-1} (C-N, str, s); ^{1}H-NMR (400 MHz, $CDCl_3$, δ ppm): 8.13-8.11 (1H, d, *J* = 8.6 Hz, *ArH*), 7.88-7.85 (2H, d, *J* = 6.52 Hz, *ArH*), 7.09-7.01 (2H, m, *ArH*), 7.00-6.96 (2H, m, *ArH*) 6.69 (1H, s, *ArH*), 4.24-4.21 (2H, t, *J* = 5.24 Hz, -CH_2), 3.89 (3H, s, -OCH_3) 3.87-3.86 (1H, t-broad, -*OH*) 3.64-3.61 (2H, m, -CH_2) 2.90-2.87 (2H, t, *J* = 5.68 Hz -CH_2), 2.65-2.55 (8H, m, -CH_2); ^{13}C NMR (100 MHz, $CDCl_3$): 177.94, 163.11, 163.00, 162.20, 157.87, 127.84, 127.06, 124.07, 116.80, 114.69, 106.07, 101.04. 66.29, 59.54, 58.01, 56.51; MS (ESI) m/z = 425.47 $[M+H]^+$, 363.56 $[M+K]^+$. $]^+$. Anal. Calcd for $C_{24}H_{28}N_2O_5$: C, 67.91; H, 6.65; N, 6.60. Found: C, 67.50; H, 6.30; N, 6.82; R_f Value: 0.15 ($CHCl_3$: MeOH, 9:1).

4.2. Biological activity

4.2.1. In vitro inhibition of AChE

The inhibitory potency of target compounds on AChE was determined using spectroscopic method of Ellman *et al*. with slight modification and was expressed as IC_{50} , that is, inhibitory concentration that reduces the cholinesterase activity by 50%.; rat cortex homogenate was used as the resource of AChE. 5,5`-dithiobis-(2-nitrobenzoic acid) (Ellman's reagent, DTNB), acetylthiocholine iodide (ATC), donepezil was purchased from Sigma Aldrich. For assay of AChE activity, a reaction mixture containing 100µl acetylthiocholine iodide 0.075M/L, 100µl sodium phosphate buffer (0.1M/L, pH 7.4), 20µl homogenate or serum and different concentrations of test compounds 20µl was incubated at 37° C for 15 min. The reaction was terminated by adding 50µl 3% sodium lauryl sulfate, then, 50µl, 0.2% of 5,5'–dithio-bis-(2-nitrobenzoic acid) was added to produce the yellow anion of 5-thio-2-nitro-benzoic acid. Assays were carried out with a blank containing all components except AChE in order to account for non-enzymatic reaction. The values of IC_{50} were calculated by UV spectroscopy from the absorbance changes at 450 nm. A positive control of donepezil was used in the same range of concentrations. Each concentration was analyzed in triplicate. Data from concentration–inhibition experiments of the inhibitors were calculated by nonlinear regression analysis, using the GraphPad Prism 5 program.

4.2.2. In vitro Advanced glycation end-product (AGEs) formation inhibitory activity

View Article Online
DOI: 10.1039/C6RA17678J

The assay for the ability of the flavone to inhibit the glucose-mediated protein glycation and the development of fluorescent AGEs was performed. Different concentrations of various compounds were prepared by dissolving in DMSO. Anti-glycation assay was performed according to the methods reported by Matsuura and colleagues with slight modification. In all experiments, about 500 µl of Bovine serum albumin (1mg/ml final concentration) was incubated with 400 µl of glucose (500 mM) in the presence of 100 µl of test compounds, aminoguanidine or PBS as control buffer at different concentrations, The reaction was allowed to proceed at 60°C for 24hrs and thereafter reaction was stopped by adding 10 µl of 100% (w/v) trichloroacetic acid (TCA). Then the mixture was kept at 4°C for 10 min before subjected to centrifugation at 15,000 rpm. The precipitate was redissolved in 1ml alkaline PBS (pH 10) and immediately quantified for relative amount of glycated BSA based on fluorescence intensity by spectrofluorometer LS-55 (Perkin Elmer) at 370 nm (excitation) and 440 nm (emission). Aminoguanidine was used as a positive control. Percentage inhibition was calculated. All experiments were performed in triplicate.[41]

4.2.3. DPPH radical scavenging activity method

The stable 1, 1-diphenyl-2-picryl hydrazyl radical (DPPH) was used for determination of free radical-scavenging activity of the test compounds. The 0.1 mM solution of DPPH in methanol (39.4 mg in 1000 ml) was freshly prepared. Different concentrations of test compounds were added with an equal volume to methanol solution of DPPH. After 30 min at room temperature, the absorbance was recorded at 517 nm. Ascorbic acid was used as standard. IC_{50} values denote the concentration of sample, which is required to scavenge 50% of DPPH free radicals. IC_{50} value was determined from the plotted graph of scavenging activity against the different concentrations of test compounds. Ascorbic acid was applied as positive drug.[42]

4.2.4. Kinetic characterization of AChE inhibition

The kinetics studies were performed using the Ellman's method with three different concentrations (0.01, 0.05 and 0.1 µM) of compound **7h**. The Lineweaver–Burk reciprocal plots were constructed by plotting the inverse initial velocity (1/V) as a function of the inverse of the substrate concentration (1/[S]) at varying concentrations of the substrate acetylthiocholine (0.05–0.5 mM). The parallel control experiments were achieved without inhibitor in the assay. The double reciprocal plots were evaluated by a weighted least-squares analysis. Each experiment was performed in triplicate.

View Article Online
DOI: 10.1039/C6RA17678J

4.2.5. Molecular docking studies

To understand the binding interactions and selectivity of our synthesized compounds against AChE, molecular docking simulation was carried out with Glide program of Schrödinger software. The compounds showing good anti-cholinesterase activity were sketched and cleaned in maestro molecular modeling workspace followed by energy minimization in '*ligprep*' program of Schrödinger software using OPLS_2005 force field at pH of 7.4 [43]. The X-ray crystallographic structure of AChE complex with donepezil (PDB code 1EVE) was obtained from the Protein Data Bank (http://www.rcsb.org/pdb) and optimized for docking analysis [44]. The optimization protocol includes addition of hydrogen atoms, deletion of water molecules, completion of bond orders, assignment of hydrogen bonds and complex minimization to RMSD of 0.20Å using OPLS_2005 force field. The active molecules were docked into the active site of the protein using extra precision (XP) docking mode of '*glide*' program.[45,46]

4.2.6. ADME property prediction

To investigate the potential of the new compounds as anti-AD agents, their ADME (Absorption, Distribution, Metabolism and Excretion) properties were predicted using QikProp program, v. 3.5 of the Schrödinger software.[34] This provided an estimate of the physicochemical properties and the bioavailability of the compounds. Various parameters such as polar surface area (PSA), solvent accessible surface area (SASA), QPPCaco (predicted apparent Caco-2 cell permeability in nm/s, CNS activity (predicted central nervous system activity on a -2 (inactive) to +2 (active) scale). QPlogBB (predicted brain/blood partition coefficient), Caco-2 cells is a model for the gut blood barrier), QPPMDCK (predicted apparent MDCK cell permeability in nm/s. MDCK cells are considered to be a good mimic for the blood–brain barrier), QPlogS (predicted aqueous solubility), QPlogKhsa (prediction of binding to human serum albumin), and percent human oral absorption (predicted human oral absorption on 0–100% scale) were calculated. The acceptability of the compounds based on the Lipinski's rule of five was also estimated from the results.[47]

4.2.7. In vivo brain AChE activity assay

4.2.7.1. Animals

View Article Online
DOI: 10.1039/C6RA17678J

Swiss albino mice of either sex weighing 20–25 g (procured from Central Research Institute, Kasauli, Himachal Pradesh, India) were used for this study. The animals were housed in the Animal house facility, Punjabi University Patiala, India and the care of the animals was carried out as per the guidelines of the Committee for the Purpose of Control and Supervision of Experiments on Animals (CPCSEA), Ministry of Environment and Forest, Government of India (Reg. No. 107/1999/CPCSEA).

4.2.7.2. Drug administration

Compound **7h** was dissolved in 10% dimethylsulfoxide (DMSO) and administered through intraperitoneal injection at doses ranging from 50 to 200 mg/kg. All other reagents used in the present study were of analytical grade and freshly prepared.

4.2.7.3 Tissue preparation for bioassay

After 48 h of intraperitoneal injection, animals were sacrificed by cervical dislocation and their brains were taken out quickly and perfused with 0.15 M NaCl until free of blood. Dissected brain was homogenized in 200 mM phosphate buffer (pH 7.7) to get 5% (w/v) homogenate. The homogenate was centrifuged at 10,000 rpm for 10 min at 4 $^{\circ}$C to separate the nuclear debris. The supernatant thus obtained was used for the estimation of activity of acetylcholinesterase. The brain acetylcholinesterase activity at different volumes of supernatant (10, 20, 30, 40 and 50 µL) with 15 µL of 1 mM ATCh was determined using Ellman method reported in section 4.2.1.

4.2.8. Molecular Dynamic Simulations

The molecule with the highest inhibitory activity docked with the AChE protein was used in molecular dynamics simulations (10 ns) using Desmond molecular dynamics module of Schrodinger.[48] The simulations aided to stabilize the protein-ligand complex and analyze the most probable interaction by studying its simulation–interaction diagram. From this analysis, the important interactions for ligand were assessed and can be utilized for further identification. For molecular dynamics simulations, the system was first built using the TIP3P solvent model with orthorhombic box shape; the pH was adjusted by adding Na^+ ions, and the salt concentration was set at 0.15 M. The simulation was carried out using the NPT ensemble and a time step of 1.0 fs; the temperature was fixed at 310 K using the Nose-Hoover Chain method as the thermostat and pressure of 1.01325 bar using Martyn–Tobias–Klein as the barostat.

View Article Online
DOI: 10.1039/C6RA17678J

Acknowledgments

I am grateful to my colleagues and assistants for this study and editorial assistance with the manuscript. We wish to thank the 'Indian Council of Medical Research (ICMR)', New Delhi, for providing us a Senior Research Fellowship (ICMR-SRF); Award No. BIC/11(11)/2014. Dr. Balraj Saini, Sophisticated Instrument Centre (SIC), Punjabi University, Patiala, and SAIF, Punjab University, Chandigarh is acknowledged for providing access to spectrofluorometer and spectral facilities.

Conflict of interest

We declare that we have no conflict of interest.

Refernces

1. M. G. Cardozo, T. Kawai, Y, Iimura, H, Sugimoto, Y. Yamanishi and A. J. Hopfinger, *J. Med. Chem.,* 1992, **35**, 590-601.
2. E. Scarpini, P. Scheltens and H. Feldman, *Lancet Neurol.,* 2003, **2**, 539-547.
3. F. Cuetos, E. Herrera and A. W. Ellis, *Neuropsychologia,* 2010, **48**, 3329-3334.
4. D. Galimberti and E. Scarpini, *CNS Neurol. Disord. Drug Targets,* 2011, **10**, 163-174.
5. P. Taupin, *Cent. Nerv. Syst. Agents Med. Chem.,* 2010, **10**, 16-21.
6. R. Sultana and D. A. Butterfield, *J. Alzheimers Dis.,* 2010, **19**, 341-353.
7. M. Singh, M. Kaur, N. Chadha and O. Silakari, *Mol. Divers.,* 2016, **20**, 271-297.
8. P. T. Francis, A. M. Palmer, M. Snape and G. K. Wilcock, *J. Neurol. Neurosurg. Psychiatry.,* 1999, **66**, 137-147.
9. M. Singh, M. Kaur, H. Kukreja, R. Chugh, O. Silakari and D. Singh, *Eur. J. Med. Chem.,* 2013, **70**, 165-188.
10. D. S. Auld, T. J. Kornecook, S. Bastianetto and R. Quirion, *Prog. Neurobiol.,* 2002, **68**, 209-245.

View Article Online
DOI: 10.1039/C6RA17678J

11. D. A. Butterfield, T. Reed, S. F. Newman and R. Sultana, *Free Radic. Biol. Med.,* 2007, **43**, 658-677.

12. M.A. Ansari, S.W. Scheff, *J. Neuropathol. Exp. Neurol.,* 2010, **69**, 155-167.

13. Y. He, P. F. Yao, S. B. Chen, Z. H. Huang, S. L. Huang, J. H. Tan, D. Li, L. Q. Gu and Z. S. Huang, *Eur. J. Med. Chem.,* 2013, **63**, 299-312.

14. W. R. Markesbery, *Free Radic. Biol. Med.,* 1997, **23**, 134-147.

15. S. Yamagishi, M. Takeuchi, Y. Inagaki, K. Nakamura and T. Imaizumi, *Int. J. Clin. Pharmacol. Res.,* 2003, **23**, 129-134.

16. S. Yamagishi and T. Imaizumi, *Curr. Pharm. Des.,* 2005, **11**, 2279-2299.

17. T. Sato, M. Iwaki, N. Shimogaito, X. Wu, S. Yamagishi and M. Takeuchi, *Curr. Mol. Med.,* 2006, **6**, 351-358.

18. M. P. Vitek, K. Bhattacharya, J. M. Glendening, E. Stopa, H. Vlassara, R. Bucala, K. Manogue and A. Cerami, *Proc. Natl. Acad. Sci. USA,* 1994, **91**, 4766-4770.

19. M. D. Ledesma, P. Bonary, C. Colaco and J. Avila, *J. Biol. Chem.,* **269**, 1994, 21614-21629.

20. S. D. Yan, X. Chen, A. M. Schmidt, J. Brett, G. Godman, Y. S. Zou, C. W. Scott, C. Caputo, T. Frappier and M. A. Smith, *Proc. Natl. Acad. Sci. USA,* 1994, **91**, 7787-7791.

21. Y. Chen, J. Sun, L. Fang, M. Liu, S. Peng, H. Liao, J. Lehmann and Y. Zhang, *J. Med. Chem.,* 2012, **55**, 4309-4321.

22. I. Tomassoli, L. Ismaili, M. Pudlo, C. de Los Rios, E. Soriano, I. Colmena, L. Gandia, L. Rivas, A. Samadi, J. Marco-Contelles and B. Refouvelet, *Eur. J. Med. Chem.,* 2011, **46**, 1-10.

23. B. Kumar, Sheetal, A. K. Mantha and V. Kumar, *RSC Adv.,* 2016, **6**, 42660-42683.

View Article Online
DOI: 10.1039/C6RA17678J

24. F. Li, Z. Wang, J. Wu, J. Wang, S. Xie, J. Lan, W. Xu, L. Kong and X. Wang, *J. Enzyme Inhib. Med. Chem.,* 2016, 1-13.

25. D. H. Kim, C. H. Yun, M. H. Kim, C. K. Naveen, B. H. Yun, J. S. Shin, H. J. An, Y. H. Lee, Y. D. Yun, H. K. Rim, M. S. Yoo, K. T. Lee and Y. S. Lee, *Bioorg. Med. Chem. Lett.,* 2012, **22**, 700-705

26. J. Greeff, J. Joubert, S. F. Malan and S. van Dyk, *Bioorg. Med. Chem.,* 2012, **20**, 809-818.

27. Y. Morimitsu, K. Yoshida, S. Esaki and A. Hirota, *Biosci. Biotechnol. Biochem.,* 1995, **59**, 2018-2021.

28. (a) M. Singh, M. Kaur and O. Silakari, *Eur. J. Med. Chem.,* 2014, **84**, 206-239; (b) I. Solanki, P. Parihar, M.L. Mansuri and M.S. Parihar, *Adv. Nutr.,* 2015, **6**, 64-72.

29. G. Kaur, M. Kaur and O. Silakari, *Mini Rev. Med. Chem.,* 2014, **14**, 747-767.

30. M. L. Bolognesi, R. Banzi, M. Bartolini, A. Cavalli, A. Tarozzi, V. Andrisano, A. Minarini, M. Rosini, V. Tumiatti, C. Bergamini, R. Fato, G. Lenaz, P. Hrelia, A. Cattaneo, M. Recanatini and C. Melchiorre, *J. Med. Chem.,* 2007, **50**, 4882-4897.

31. W. Baker, *J. Chem. Soc.,* 1933, **10**, 1381-1389.

32. H. S. Mahal and K. J. Venkataraman, *J. Chem. Soc.,* 1934, **56**, 1767-1769.

33. G. L. Ellman, K. D. Courtney, A Valentino and R. M. Featherstone, *Biochem. Pharmacol.,* 1961, **7**, 88-95.

34. N. Matsuura, T. Aradate, C. Sasaki, H. Kojima, M. Ohara, J. Hasegawa and M. Ubukata, *J. Health Sci.,* 2002, **48**, 520-526.

35. J. L. Sussman, M. Harel, F. Frolow, C. Oefner, A. Goldman, L. Toker and I. Silman, *Science,* 1991, **53**, 872-879.

View Article Online
DOI: 10.1039/C6RA17678J

36. QikProp, Version 3.5; Schrödinger, LLC: New York, NY, 2012.

37. J. Kelder, P. D. Grootenhuis, D. M. Bayada, L. P. Delbressine and J. P. Ploemen, *Pharm. Res.,* 1999, **16**, 1514-1519.

38. F. Hobbiger and R. Landaster, *J. Neurochem.,* 1971, **18**, 1741-1749.

39. J. B. Shaik, B. K. Palaka, M. Penumala, K. V. Kotapati, S. R. Devineni, S. Eadlapalli, M. M. Darla, D. R. Ampasala, R. Vadde and G. D. Amooru, *Eur. J. Med. Chem.,* 2016, **107**, 219-232.

40. W. Luo, Y. B. Su, C. Hong, R. G. Tian, L. P. Su, Y. Q. Wang, Y. Li, J. J. Yue and C. J. Wang, *Bioorg. Med. Chem.,* 2013, **21**, 7275-7282.

41. A. Prathapan, S.V. Nampoothiri, S. Mini, K.G. Raghu*, Eur. Rev. Med. Pharmacol. Sci.* 2012, **16**, 57-65.

42. M. S. Blois, *Nature,* 1958, **181**, 1199-1200.

43. Ligprep, version 2.5; Schrodinger, LLC, New York, 2011.

44. G. Kryger, I. Silman and J. L. Sussman, *Structure,* 1999, 7, 297-307.

45. Glide, version 5.6; Schrodinger, LLC, Newyork, NY, 2010.

46. R. A. Friesner, J. Banks, R. B. Murphy, T. A. Halgren, J. J. Klicic, D. T. Mainz, M. P. Repasky, E. H. Knoll, D. E. Shaw, M. Shelley, J. K. Perry, P. Francis and P. S. Shenkin*, J. Med. Chem.,* 2004, 47, 1739-1749.

47. C. A. Lipinski, F. Lombardo, B. W. Dominy and P. J. Feeney, *Adv. Drug Deliv. Rev.,* 2001, **46**, 3-26.

48. K. J. Bowers, E. Chow, H. Xu, R. O. Dror, M. P. Eastwood, B. A. Gregersen, J. L. Klepeis, I. Kolossvary, M. A. Moraes and F. D. Sacerdoti, Scalable algorithms for

View Article Online
DOI: 10.1039/C6RA17678J

molecular dynamics simulations on commodity clusters, In: SC 2006, Conference, Proceedings of the ACM/IEEE. IEEE, pp 43-43.

View Article Online
DOI: 10.1039/C6RA17678J

Figure Captions

Figure 1: FDA approved drugs for the treatment of Alzheimer's disease.

Figure 2: Lineweaver–Burk plot from the substrate–velocity curves of the AChE activity with different substrate concentrations (0.05–0.5 mM) in the absence and presence of compound **7h** at 2, 5 and 10 μM.

Figure 3: Docked pose of interactions of compounds **7k** and **7h** with AChE active site (1EVE) using Glide. (**A**) 2D representation of different interactions of **7k** with TcAChE. (**B**) 3D representation of different interactions of compound **7k** with residues in the binding sites of TcAChE. The compound is rendered in green stick model and the residues are rendered in blue sticks. Hydrogen bonds are indicated with green dashed lines. Residues involved in hydrophobic interactions with the ligand are shown with dashed lines. (**C**) The TcAChE enzyme is depicted in surface view and compound **7k** as stick in the binding pocket. (**D**) 2D representation of different interactions of **7h** with TcAChE generated using Glide. (**B**) 3D representation of different interactions of compound **7h** with residues in the binding sites of TcAChE. (**C**) The TcAChE enzyme is depicted in surface view and compound **7h** as stick in the binding pocket.

Figure 4: post-MD hydrogen bonds and hydrophobic interactions of **7h** with AChE

Scheme 1: Synthetic scheme for the of 2-phenyl-1-benzopyran-4-one derivatives **7(a–k)**.

Table 1: The AChE inhibition, Radical scavenging activities and advanced glycation end products (AGEs) formation inhibitory activity data **7(a-k)**.

View Article Online
DOI: 10.1039/C6RA17678J

Table 1: The AChE inhibition, Radical scavenging activities and advanced glycation end products (AGEs) formation inhibitory activity **7(a-k)**.

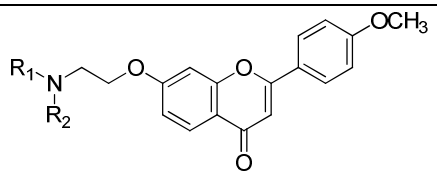

C. No.	-NR_1R_2	AChE Inhibitory Activity (IC_{50}[b] ±SD[a], nM)	Radical scavenging activity (EC_{50}[c]± SD[a], nM)	AGEs Inhibitory Activity (IC_{50}[d]± SD[a], µM)
7a	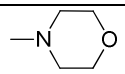	11.0±0.30	54.33±1.13	56.33±0.94
7b	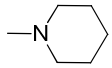	21.76±0.70	48.43±0.83	64.03±1.90
7c	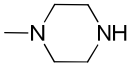	51.00±1.40	30.5±2.19	72.92±1.25
7d	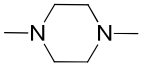	31.06±2.87	45.46±0.96	51.16±1.40
7e		104.83±2.74	69.46±2.05	80.23±2.21
7f		27.1±1.16	49.1±1.44	50.36±0.65
7g		77.46±1.06	92.26±1.46	75.23±1.02
7h	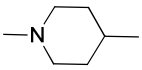	6.33±0.98	24.66±1.12	43.53±0.85
7i	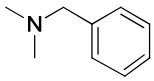	36.5±0.92	34.2±1.57	69.33±2.04
7j	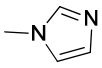	108.3±3.99	87.13±1.58	113.14±1.05
7k	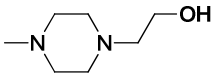	7.56±1.17	21.56 ±1.20	36.76±1.51
Std.	Donepezil	12.7±0.20	-	
Std.	Ascorbic acid	-	20.0± 0.54	
Std.	Aminoguanidine (AG)	-	-	40.06±1.78

[a] SD: Data are expressed as mean ± SD (n=3). Data were statistically analyzed by one way ANOVA; *P<0.05 vs Std.

[b] IC_{50} , inhibitor concentration (means ± SD of three experiments) for 50% inactivation of AChE.

[c] EC_{50} was defined as the effective concentration resulting in 50% scavenging activity.

[d] IC_{50} was defined as the concentration resulting in 50% inhibition of AGEs product formation.

View Article Online
DOI: 10.1039/C6RA17678J

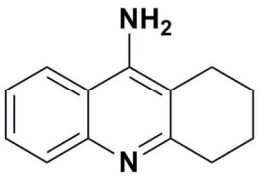

Tacrine (1993)

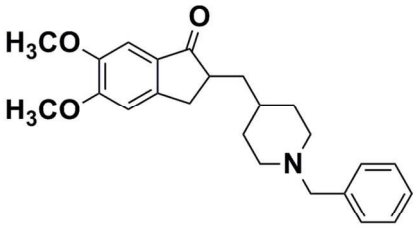

Donepezil (1996)

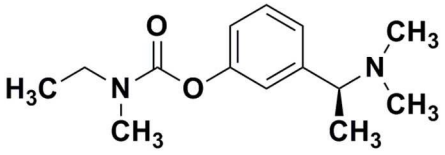

Rivastigmine (2000)

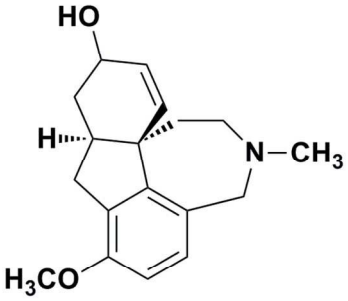

Galantamine (2001)

FDA approved drugs for the treatment of Alzheimer's disease.

122x90mm (300 x 300 DPI)

View Article Online
DOI: 10.1039/C6RA17678J

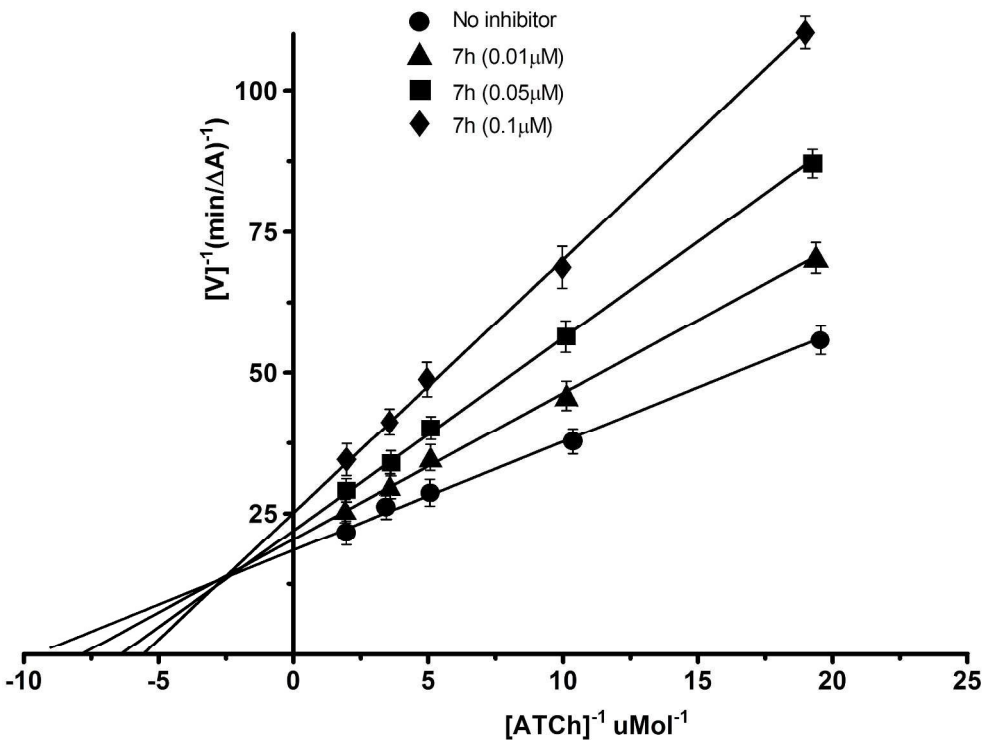

Lineweaver–Burk plot from the substrate–velocity curves of the AChE activity with different substrate concentrations (0.05–0.5 mM) in the absence and presence of compound 7h at 2, 5 and 10 μM.

768x575mm (96 x 96 DPI)

View Article Online
DOI: 10.1039/C6RA17678J

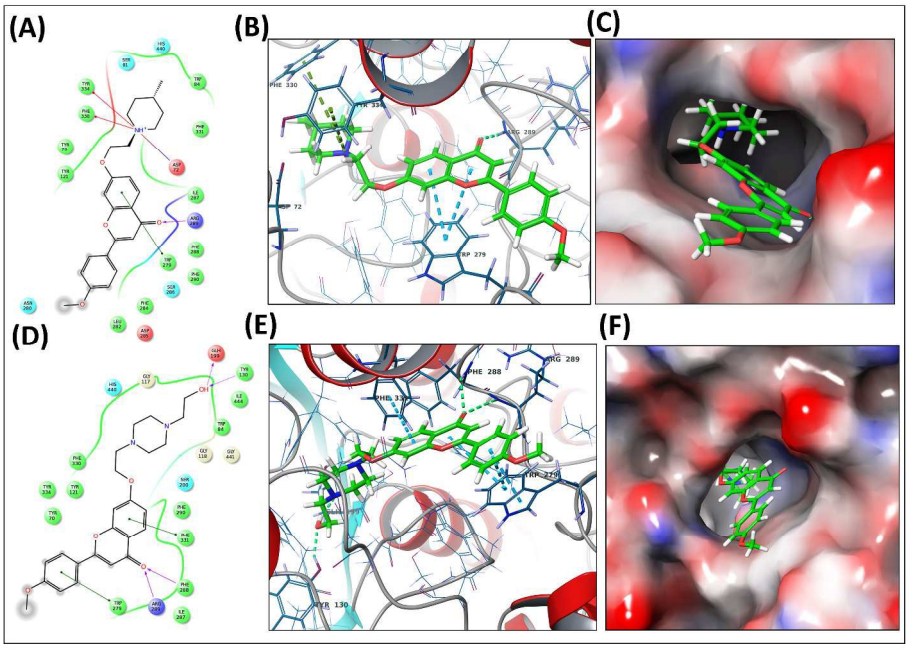

Docked pose of interactions of compounds 7k and 7h with AChE active site (1EVE) using Glide. (A) 2D representation of different interactions of 7k with TcAChE. (B) 3D representation of different interactions of compound 7k with residues in the binding sites of
TcAChE. The compound is rendered in green stick model and the residues are rendered in blue sticks. Hydrogen bonds are indicated with green dashed lines. Residues involved in hydrophobic interactions with the ligand are shown with dashed lines. (C) The TcAChE enzyme is depicted in surface view and compound 7k as stick in the binding pocket. (D) 2D representation of different interactions of 7h with TcAChE generated using Glide. (B) 3D representation of different interactions of compound 7h with residues in the binding sites of TcAChE. (C) The TcAChE enzyme is depicted in surface view and compound 7h as stick in the binding pocket.

279x215mm (300 x 300 DPI)

View Article Online
DOI: 10.1039/C6RA17678J

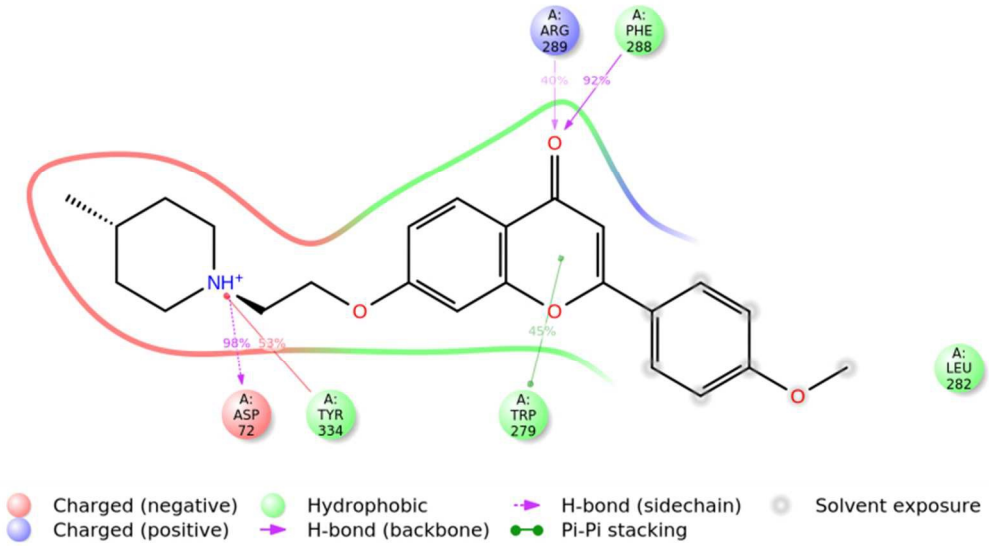

post-MD hydrogen bonds and hydrophobic interactions of 7h with AChE

219x123mm (96 x 96 DPI)

View Article Online
DOI: 10.1039/C6RA17678J

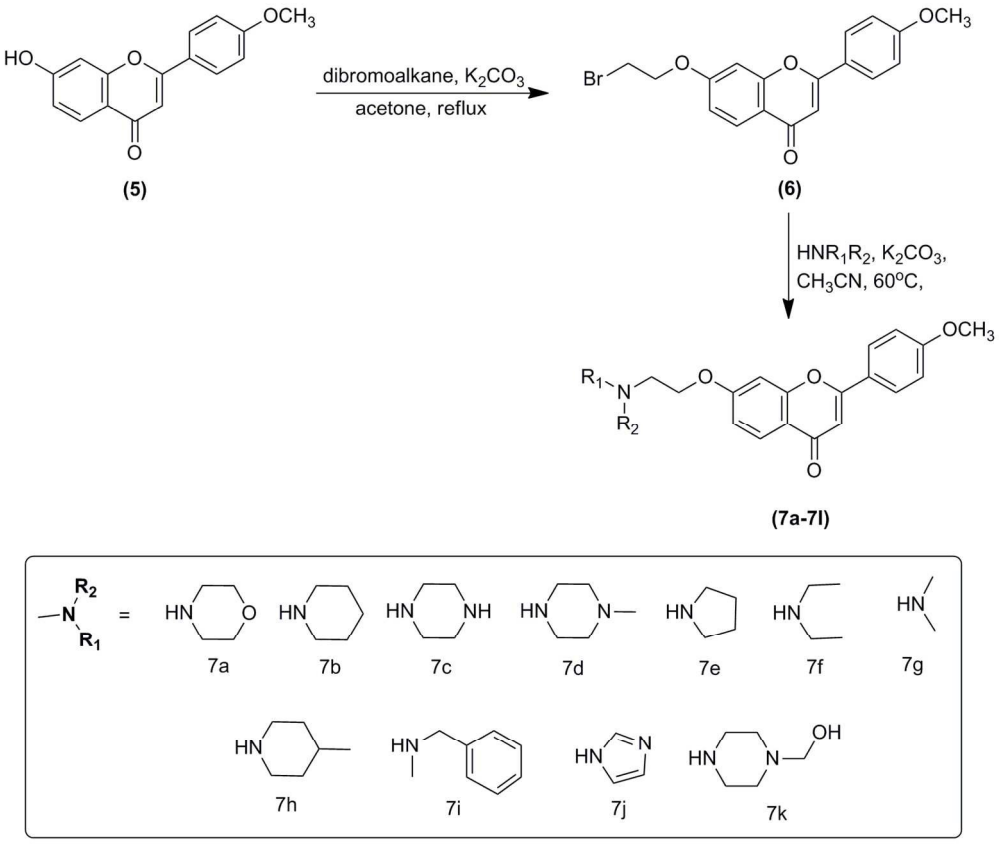

Synthetic scheme for the of 2-phenyl-1-benzopyran-4-one derivatives 7(a–k).

140x118mm (300 x 300 DPI)

View Article Online
DOI: 10.1039/C6RA17678J

Graphical Abstract

Design, Synthesis and Biological Evaluation of Novel 2-phenyl-1-benzopyran-4-one Derivatives as potential poly-functional anti-Alzheimer's agents

Manjinder Singh, Om Silakari,*

ABSTRACT:

Development of Multi-Target Directed Ligands (MTDLs) has emerged as a promising approach for targeting complex etiology of Alzheimer's disease (AD). Following this approach, a new series of 2-phenyl-1-benzopyran-4-one derivatives were designed, synthesized and biologically evaluated as inhibitors of acetylcholinesterases (AChEs), advanced glycation end products formation (AGEs) and also for their radical scavenging activity. These 2-phenyl-1-benzopyran-4-one derivatives might be the promising lead compound as potential poly-functional anti-Alzheimer's agents.